Published as: *Cancer Discov*. 2015 February ; 5(2): 168–181.

Aberrant glycosylation promotes lung cancer metastasis through adhesion to galectins in the metastatic niche

Nathan E. Reticker-Flynn[1,2] and **Sangeeta N. Bhatia**[1,2,3,4,5,*]

[1]David H. Koch Institute for Integrative Cancer Research, Massachusetts Institute of Technology, Cambridge, Massachusetts 02139, USA

[2]Harvard-MIT Division of Health Sciences and Technology, Massachusetts Institute of Technology, Cambridge, Massachusetts 02139, USA

[3]Howard Hughes Medical Institute, Cambridge, Massachusetts 02139, USA

[4]Division of Medicine, Brigham and Women's Hospital, Boston, Massachusetts 02115, USA

[5]Department of Electrical Engineering and Computer Science, Massachusetts Institute of Technology, Cambridge, Massachusetts 02139, USA

Abstract

Metastasis is the leading cause of cancer-associated deaths. While dissemination of tumor cells likely occurs early in tumorigenesis, the constituents of the microenvironment play essential rate-limiting roles in determining whether these cells will form clinically-relevant tumors. Recent studies have uncovered many molecular factors that contribute to establishment of a pro-tumorigenic metastatic niche. Here, we demonstrate that galectin-3, whose expression has clinical associations with advanced malignancy and poor outcome, contributes to metastatic niche formation by binding to carbohydrates on metastatic cells. We show that galectin-3 is expressed early during tumorigenesis by both $CD11b^{+}Gr\text{-}1^{+}$ and $CD11b^{+}Ly\text{-}6C^{hi}$ leukocytes. Tumors mobilize these myeloid populations through secretion of soluble factors including IL-6. We find that metastatic cancer cells exhibit elevated presentation of the oncofetal galectin-3 carbohydrate ligand, the Thomsen-Friedenreich Antigen, on their surfaces as a result of altered C2GnT2 and St6GalNAcIV glycosyltransferase activity that inhibits further glycosylation of this carbohydrate motif and promotes metastasis.

Keywords

NSCLC; metastasis; glycosylation; glycosyltransferase; galectin-3; IL-6; Thomsen-Friedenreich Antigen; *St6galnac4*; *Gcnt3*; tumor microenvironment

[*]To whom correspondence should be sent: S. Bhatia, 77 Massachusetts Ave, Building 76-453, Cambridge, MA 02139, sbhatia@mit.edu, phone: 617-324-0221, fax: 617-324-0740.

The authors have no conflicts of interest to disclose.

Authors' Contributions

S. Bhatia and N. Reticker-Flynn designed the studies and wrote the manuscript. N. Reticker-Flynn performed all experiments and data analysis.

Introduction

Galectins are a family of β-galactoside binding lectins whose pleiotropic roles in tumorigenesis have been reported to range from interactions with oncoproteins, to immunomodulation, to promotion of angiogenesis, to eliciting anti-apoptotic effects through BCL2 homologies (1–3). Despite the fact that galectins lack a signal sequence or transmembrane domain, they can be incorporated into the extracellular matrix (ECM), secreted as soluble factors into circulation, presented on cell surfaces, or act intracellularly. In particular, the presence of galectin-3 as an extracellular molecule (circulating in serum or localized on cells within tissues) has been associated with metastasis. Elevated levels of galectin-3 have been reported in patients with advanced stages of a variety of cancers (4, 5), and treatment of mice bearing xenograft tumors with a truncated form of the protein that acts as a competitive binding inhibitor has been reported to reduce incidences of metastases (6). In particular, galectin-3 and galectin-8 contain carbohydrate recognition domains (CRDs) that exhibit specific affinities for the oncofetal core 1 *O*-linked disaccharide termed the Thomsen-Friedenreich Antigen (T-Antigen) (7–9). While this mucin-type glycan motif forms the core structure of most *O*-glycans (Galβ1-3GalNAcα1-Ser/Thr), exposure of the disaccharide form is generally occluded by further glycosylation. It is estimated, however, that the cells in as many as 90% of carcinomas express this disaccharide without further glycosylation (10). Nonetheless, the mechanisms by which this conserved glycan motif is regulated by cancer cells, along with the precise role that it plays in tumorigenesis and metastasis, are poorly understood.

Recently, the role that dynamic remodeling of the tumor microenvironment plays in the promotion of metastasis has been partially elucidated (11–13). Soluble factors released from tumors act to mobilize bone marrow-derived cells (BMDCs), and in particular myeloid cells, into the peripheral blood and recruit them to the early metastatic niche, a site where metastases have yet to reach a detectable size. Frequently, these myeloid cells consist of $CD11b^{+}$ cells that are Ly-$6C^{hi}$ or Gr-1^{+}. The former population typically consists of inflammatory monocytes, while the latter may represent neutrophils or a heterogeneous poorly differentiated granulocyte population that exhibits suppressor functions, sometimes referred to as myeloid-derived suppressor cells (MDSCs). Crosstalk between primary or metastatic tumors and these or other non-parenchymal populations induce the secretion of factors in autocrine, paracrine, and endocrine fashions in a manner that promotes remodeling of the primary tumor, bone marrow, and metastases to promote malignant progression. Among the molecules that are involved in metastatic niche formation, many are extracellular matrix (ECM) molecules and their modifiers including fibronectin, collagen IV, tenascin-c, osteopontin, periostin, versican, lysyl oxidase (LOX), and a variety of matrix metalloproteinases (MMPs) (14–21). The role of cell-surface galectins, however, as components of the early metastatic niche, remains to be investigated.

Alterations in gene expression, cytokine secretion, and ECM and soluble factor production have all been associated with improved interactions between metastatic cells and specific microenvironments (14–16, 18, 19, 22–26). To determine the involvement of galectin-3 within the metastatic niche and of aberrant glycosylation of cancer cell-associated surface glycoproteins, we used a mouse model of lung adenocarcinoma metastasis (27–29).

Previously, we used our ECM microarray platform to identify adhesion ligands associated with metastasis and identified galectin-3 and -8 as exhibiting preferential adhesion to metastatic cells (30). Here, we identify galectin-3 as a component of the metastatic niche through expression on myeloid cells. We find that changes in glycosylation by the cancer cells mediate their increased interactions with galectins, and that these alterations play essential roles in conferring metastatic potential. In particular, we find that the upregulation of the sialyltransferase St6GalNAcIV and downregulation of the core 2 *N*-acetylglucosaminyltransferase C2GnT2 (*Gcnt3*) are key mediators of the changes in glycosylation that potentiate metastatic proclivity by preserving presentation of the T-Antigen.

Results

Tumor-bearing mice exhibit elevated levels of galectin-3 in the early metastatic niche

To determine the role of galectin-3 in metastasis, we used a genetic mouse model of lung adenocarcinoma metastasis (*Kras*$^{LSL\text{-}G12D/+}$;*p53*$^{flox/flox}$) from which cell lines representing distinct stages of metastatic progression were derived(27–29). Following Cre-mediated recombination and the development of autochthonous lung tumors and metastases, lines were generated from primary tumors that did not give rise to metastases (T_{nonMet}), did give rise to metastases (T_{Met}), lymph node metastases (N), and liver metastases (M). Previously, we found that increasingly metastatic lines exhibited increased adhesion to galectin-3 *in vitro* (Fig. 1A) (30). As ECM molecules and their modification by BMDCs play important roles in the development of the metastatic niche, we asked whether galectin-3 has a role in its establishment. Livers were harvested from tumor-bearing mice prior to the detection of overt metastases, and examined for accumulation of galectin-3. Western blot analysis of liver protein lysates revealed an elevation in galectin-3 in the livers of tumor-bearing mice compared to naïve mice (Fig. 1B). To identify the source of this galectin, we examined both the tumor cells and recruited leukocytes. Gene expression microarray and western blot analyses of galectin-3 in the tumor cell lines revealed equivalent expression of the molecules across all four classes of lines, indicating that galectin-3 expression by tumors is not differentially regulated during tumor progression (Supplementary Fig. 1A, B). In light of recent reports of myeloid-derived populations supporting outgrowth of metastatic tumors, however, we asked whether such populations might also be presenting galectin-3 within the early metastatic niche. Staining for macrophages and galectin-3 in liver sections of mice bearing either T_{nonMet} or M tumors but no detectable overt metastases revealed colocalization of galectin-3 with F4/80^{pos} macrophages (Fig. 1C). While galectin-3^{pos} macrophages are present in the livers of tumor-free mice as well, their numbers are two to four times lower than observed in tumor-bearing mice (Fig. 1C). Furthermore, immunostaining of the engrafted tumors also revealed a dense macrophage infiltration that colocalized with galectin-3 staining (Supplementary Fig. 1C). While other sources of galectin-3 could include secretion directly by the tumors, these findings suggested the possibility that leukocytes might be expressing galectin-3, themselves.

Tumor-bearing mice exhibit circulating CD11b$^+$galectin-3$^+$ myeloid cells early in tumorigenesis

Given our observation of galectin-3 expressing macrophages in the metastatic niche, we asked whether tumors induce the mobilization of leukocytes expressing galectin-3. We harvested peripheral blood from naïve mice or mice bearing tumors generated by either T_{nonMet} or M lines (Supplementary Fig. 2A–C) and analyzed it for the presence of galectin-3$^+$ and CD11b$^+$ myeloid cells. Analysis of peripheral blood cells by flow cytometry revealed a marked increase in galectin-3$^+$ and CD11b$^+$ leukocytes in the circulation of mice bearing both the M and T_{nonMet} tumors (Fig. 2A–C and Supplementary Fig. 2D–F). Consistent with the findings of galectin-3$^+$ macrophages in the liver, there was an enrichment in galectin-3$^+$CD11b$^+$ double-positive populations in the blood of tumor-bearing mice (Fig. 2A,D). In agreement with previous reports of increases in inflammatory myeloid cells in tumor-bearing mice, there was a significant increase in the frequency of CD11b$^+$Gr-1$^+$ and CD11b$^+$Ly-6C^{hi} populations (Fig. 2E,F and Supplementary Fig. 2G,H), which may represent neutrophils or MDSCs and inflammatory monocytes (IMs), respectively, with the latter population being CD115$^+$ (Supplementary Fig. 2I). Comparisons of the galectin-3 levels on the CD11b$^+$Ly-6C^{hi} and CD11b$^+$Ly-6C^{lo} populations reveal three- to four-fold higher expression on the enriched population (Fig. 2G). In contrast, galectin-3 levels on the various subpopulations of CD11b$^+$ leukocytes were not affected by the presence of tumors (Supplementary Fig. 3A–C), suggesting that there is increased mobilization of multiple galectin-3$^+$ populations into the circulation rather than increased expression on individual leukocytes.

Galectin-3 has been reported to bind a variety of macrophage cell-surface glycoproteins (31). To determine whether the galectin-3 is bound to leukocytes through carbohydrate interactions or is presented in a manner that still permits interactions with the carbohydrate recognition domain (CRD), we isolated CD11b$^+$ cells from the blood of tumor-bearing mice and incubated them in the presence of a competitive galectin-3 ligand, lactose, or a control, sucrose. Subsequent analysis revealed no significant difference in galectin-3 binding suggesting that galectin-3 is presented on the surfaces of these populations in a carbohydrate-independent manner, thus preserving the availability of the CRD to interact with other glycan ligands (Supplementary Fig. 4). Taken together, these data support the hypothesis that the presence of tumors induces the mobilization of CD11b$^+$galectin-3$^+$ myeloid-derived cells to the blood and that these leukocytes present galectin-3 in a manner that permits additional carbohydrate interactions with the lectin.

Tumor-derived interleukin 6 mobilizes CD11b$^+$galectin-3$^+$ leukocytes into the peripheral blood

Tumor-derived soluble factors frequently induce the mobilization and recruitment of pro-metastatic CD11b$^+$ populations (17, 19, 20, 25, 26, 32). To determine whether tumor-secreted factors were responsible for the observed mobilization of CD11b$^+$galectin-3$^+$ populations, we collected conditioned media (CM) from the cell lines and injected it into the circulation of wild-type mice. Two hours following injection of the CM, we harvested peripheral blood and analyzed the populations by flow cytometry. This analysis revealed pronounced increases in circulating CD11b$^+$galectin-3$^+$ leukocytes and relevant

subpopulations (Fig. 3A and Supplementary Fig. 5A–D). Again, differences in the level of galectin-3 expression on individual cells were not detectable in the peripheral blood between the two conditions (Supplementary Fig. 5E), suggesting that the elevated galectin-3 levels were due to increased mobilization of galectin-3^+ populations rather than increased expression of galectin-3 by the mobilized leukocytes.

Soluble galectin-3 has been reported to act as a chemoattractant for macrophages, monocytes, and neutrophils(1, 33, 34). The galectin-3 that we have observed has primarily been presented on the surfaces of leukocytes (Fig. 1C and 2). As the tumors also secrete galectin-3, however, we asked whether galectin-3 itself is capable of inducing the rapid mobilization of $CD11b^+$galectin-3^+ leukocytes. Injections of recombinant murine galectin-3 in control medium, however, failed to elicit any increased mobilization of the $CD11b^+$galectin-3^+ populations (Fig. 3A and Supplementary Fig. 5). Nonetheless, it is possible that galectin-3 might act in combination with other secreted factors to mobilize these populations. To determine whether galectin-3 is necessary to induce mobilization, we knocked down galectin-3 in the M line using short hairpins (Supplementary Fig. 6A). While this knockdown reduced the CM concentrations of galectin-3 by approximately 80%, there was no observable difference in the mobilization of any of the galectin-3^+ leukocytes or their surface levels of galectin-3 (Fig. 3B and Supplementary Fig. 6B–F). Furthermore, mice bearing tumors formed by the knockdown lines exhibited no differences in circulating galectin-3^+ leukocytes in the peripheral blood or the number of galectin-$3^{pos}F4/80^{pos}$ macrophages in their livers (data not shown and Supplementary Fig. 6G). Taken together, these data suggest that tumor-derived galectin-3 has no effect on the mobilization of galectin-3^+ leukocytes or their presentation of galectin-3, nor does it act in an autocrine fashion on tumor cells to induce secretion of other inflammatory cytokines.

While galectin-3 does not affect mobilization of leukocytes, we asked whether its expression by metastatic cells is necessary for seeding or colonization. To determine whether tumor-derived galectin-3 acts in a cell-autonomous manner to support growth of disseminated tumor cells, we performed experimental metastasis assays with the galectin-3 knockdown lines. Two weeks following intrasplenic inoculation of tumor cells, we queried mice for hematogenous dissemination to the liver and subsequent colonization. Analysis of GFP^+ tumor nodules on livers of mice injected with the M cell line containing the shRNAs revealed no differences in metastasis formation between the control hairpin (shLuc) and the galectin-3 hairpins (Supplementary Fig. 6H), suggesting that galectin-3 production by the metastases does not affect colonization. Thus, any interactions with galectin-3 that promote metastasis likely result from its expression by stromal populations.

Based on the observation that galectin-3-deficient tumors are still capable of inducing myeloid cell mobilization into circulation, we investigated whether other tumor-derived factors might elicit this mobilization. We next asked whether the tumors produce other cytokines or chemokines that may recruit the leukocytes. Analysis of the CM by Luminex ELISA revealed elevated levels of interleukin 6 (IL-6) compared to control medium (Fig. 3C). IL-6 is a pleotropic cytokine known to act upon multiple leukocyte subsets. As the T_{nonMet} line also elicited myeloid cell mobilization, we examined *Il6* gene expression levels in all of the cell lines from each of the four groups (Fig. 3D). Analysis of gene expression

microarray data revealed constant expression of *Il6* across all four classes of cell lines, suggesting that expression of IL-6 by tumors commences early in tumorigenesis.

To determine the relevance of tumor-derived IL-6 to the human disease, we examined genomic amplification of the *IL6* gene in patients with lung adenocarcinomas. Compared to normal blood or lung, lung adenocarcinomas had significantly elevated copy numbers of the *IL6* gene (Fig. 3E, $P = 5.04 \times 10^{-27}$). Thus, we asked whether IL-6 induces the mobilization of the galectin-3$^+$ leukocytes in our system. In contrast to galectin-3, injections of recombinant IL-6 induced the rapid mobilization of CD11b$^+$galectin-3$^+$ leukocytes and the relevant subpopulations into the circulation in a manner that mirrored CM injections (Fig. 3F,G and Supplementary Fig. 7A–D). To identify the set of leukocytes responsible for galectin-3 presentation, we analyzed the granulocytes, as they may represent a large portion of the mobilized CD11b$^+$Gr-1$^+$ cells. Thus, we repeated the IL-6 experiments in *Csf3r* (G-CSF-R) knockout mice, which exhibit impaired granulocyte production and maturation. While IL-6 was still capable of inducing CD11b$^+$Ly-6C^{hi} cell mobilization, *Csf3r*$^{-/-}$ mice exhibited a profound reduction in CD11b$^+$galectin-3$^+$ and CD11b$^+$Gr-1$^+$ leukocytes compared to wild-type mice (Supplementary Fig. 8A–D). These findings suggest that tumor-derived IL-6 is sufficient to induce mobilization of galectin-3$^+$ leukocytes.

To determine whether galectin-3 expression by the myeloid cells or another non-parenchymal population is a prerequisite to their mobilization into circulation, we repeated the IL-6 injections in *Lgals3* (galectin-3) knockout mice and observed no differences in CD11b$^+$ myeloid cell mobilization compared to wild-type mice (Fig. 3H and Supplementary Fig. 9A–E). The relevant subpopulations also demonstrated similar mobilization (Supplementary Fig. 9A–D). Taken together these data suggest that IL-6, and not galectin-3, acts systemically as a factor to induce the mobilization of CD11b$^+$galectin-3$^+$ leukocytes from the bone marrow and that display of galectin-3 by the BMDCs is not a prerequisite to their mobilization.

Increasingly metastatic cells exhibit elevated T-Antigen surface presentation that mediates galectin-3 binding

Our previous studies demonstrated that cells increase their adhesion to galectin-3 as they gain metastatic potential (30). In light of the enrichment of galectin-3$^+$ leukocytes in the peripheral blood (Fig. 2) and metastatic niche (Fig. 1D), we asked how the metastatic populations achieve enhanced adhesion to galectin-3. As galectins bind β-galactoside glycans through their carbohydrate recognition domain (CRD), we asked whether changes in glycan presentation by tumor cells confer their adhesion to galectin-3 on recruited leukocytes during metastasis. Analysis of glycan microarray datasets (35) and existing literature reveal a variety of carbohydrate ligands for these galectins (Fig. 4A). While all galectins bind lactosamines, galectin-3 exhibits specific affinities for the Thomsen-Friedenreich Antigen (T-Antigen, Galβ1-3GalNAcα1-Ser/Thr), a pan-carcinoma marker expressed on many glycoproteins (Fig. 4B) (36). Galectin-3 is unable to interact with the T-Antigen if the disaccharide is further glycosylated. Thus, we asked whether metastatic cells exhibit elevated T-Antigen levels on their surfaces that might mediate interactions with galectin-3. Staining of T_{nonMet}, T_{Met}, and M lines with a T-Antigen-specific lectin, peanut

agglutinin (PNA), revealed that the levels of T-Antigen surface presentation (~20 fold increase) correlate with metastatic potential (Fig. 4C and Supplementary Fig. 10A). To determine whether metastatic cell adhesion to galectin-3 is indeed carbohydrate mediated, we incubated the cells with fluorescent galectin-3 in the presence of a competitive binder, *N*-Acetyllactosamine (LacNAc). Flow cytometry revealed a reduction in binding in the presence of LacNAc compared to control (sucrose), suggesting that galectin-3 adhesion to the metastatic cells is carbohydrate mediated (Fig. 4D).

To investigate whether these alterations are observed in the human disease, we stained human NSCLC tissue microarrays of 100 tissue samples with PNA to assess the presence of the T-Antigen. This staining revealed elevated levels of cell-surface T-Antigen presentation in cancerous tissue compared to non-cancerous tissue, with a notable enrichment in the lymph node metastases (Fig. 4E,F and Supplementary Fig. 10B). Additionally, we examined four common NSCLC cell lines for their relative expression of the T-Antigen. Flow cytometry revealed that, indeed, three of the four lines bound PNA at comparable levels to the M line, with the most invasive of the lines, A549 (37), exhibiting the highest degree of staining (Fig. 4G). Taken together, these data suggest that lung tumors bind galectin-3 through carbohydrate epitopes, such as the T-Antigen, and that this epitope is expressed more highly on metastatic cells.

Differential gycosyltransferase expression promotes increased T-Antigen presentation through reduction of glycan chain elongation and increased capping

A variety of *O*-linked glycoproteins, such as MUC1, can exhibit profound degrees of *O*-glycosylation, and differential regulation of such glycoproteins can significantly alter the overall glycan presentation of cells. Thus, we asked whether increased T-Antigen expression is a result of upregulation of individual glycoproteins or altered glycosyltransferase activity. We isolated cell membrane proteins from T_{nonMet}, T_{Met}, and M lines and performed PNA lectin blots. These revealed a global increase in T-Antigen expression across many glycoproteins in the increasingly metastatic cells, as opposed to PNA labeling of a specific glycoprotein (Fig. 5A).

In light of this broad distribution in glycosylation, we investigated alterations in the expression and activity of glycosyltransferases. Analysis of gene expression microarrays for 216 glycosyltransferase genes did not demonstrate widespread shifts in expression, nor were there significant changes in the subset of genes that encode transferases specific for generation of the galectin-3 ligands (Supplementary Fig. 11A, B). Comparisons between the averages for the primary tumor and metastasis-derived cell lines, however, identified *Gcnt3* and *St6galnac4* as being under- and over-expressed in the metastatic lines, respectively (Fig. 5B); these alterations were confirmed by qRT-PCR in the representative cell lines (Fig. 5C, top). C2GnT2 (*Gcnt3*) induces the addition of a β(1-6)GlcNAc to the T-Antigen, whereas St6GalNAcIV adds an α(2-6)NeuAc to the sialyl-T-Antigen (Fig. 5C, bottom). As further elongation of the core 1 disaccharide prevents binding by galectin-3 (Fig. 4B), changes in transferase activity consistent with the expression changes in *Gcnt3* and *St6galnac4* would promote T-Antigen presentation through prevention of branching and capping of elongation, respectively. Gene expression microarray analysis of the other cell lines of each class

revealed similar trends for these and analogous transferases (Supplementary Fig. 12). Consistent with the fact that generation of the T-Antigen occurs in the Golgi prior to subsequent glycosylation (38), no difference in T-Antigen blotting was visible between whole cell lysates of T_{Met} and M lines (Supplementary Fig. 13A), further confirming that differences in its presentation are due to decreased glycan extension rather than increased production of the disaccharide.

To determine the relevance of the capping and branching transferases to human disease, we again examined copy number of the *GCNT3* gene in the human TCGA lung cancer datasets. This analysis revealed a decrease in copy number in lung adenocarcinoma compared to normal blood or lung (Fig. 5D, $P = 1.44 \times 10^{-11}$). Additionally, we examined gene expression of the relevant glycosyltransferase genes in the four human NSCLC cell lines that exhibited varying degrees of PNA staining. While minimal differences in expression were observed for the transferases that give rise to the core disaccharide (*C1GALT1* and *C1GALT1C1*), there were marked variances across the lines for the genes encoding transferases that produce the branched and capped structures (Supplementary Fig. 13B). These data suggest that alterations in glycosyltransferase activity that regulate capping or branching of the T-Antigen may also pertain to the human disease.

Regulation of *Gcnt3* and *St6galnac4* mediate galectin-3 adhesion *in vitro* and metastasis *in vivo*

To test the functional role of these transferases on galectin-3 binding and metastasis, we transfected the metastatic cells with *Gcnt3* or knocked down *St6galnac4* with short hairpins. Transfection of *Gcnt3* resulted in decreased T-Antigen presentation and decreased galectin-3 binding, and, in a complementary fashion, knockdown of *St6galnac4* yielded a reduction in galectin-3 binding, while having no effect on non-sialylated T-Antigen presentation (as PNA does not recognize sialylated forms of the antigen) (Fig. 6A and Supplementary Fig. 14A–E, 15A, B). To determine the functional role of St6GalNAcIV activity on metastasis *in vivo*, we performed experimental metastasis assays with the *St6galnac4* knockdown line. Cells expressing a hairpin for the sialyltransferase or a control hairpin against firefly luciferase were injected into the spleens of mice and monitored for liver tumor formation following hematogenous dissemination. We found that mice injected with the 393M1-sh*St6galnac4* cells exhibited greater than 95% fewer liver metastases than control mice two weeks following tumor cell injection (Fig. 6B,C and Supplementary Fig. 16). We observed no differences in proliferation rates between the knockdown and control hairpin cell lines *in vitro* (Supplementary Fig. 17). Taken together, these data suggest that alterations in glycosyltransferase activity observed in increasingly metastatic cells have a functional impact on the metastatic potential of the tumor cells and support the hypothesis that presentation of the T-Antigen, through the prevention of further glycosylation, promotes adhesion of tumor cells to galectin-3 in the metastatic niche.

Discussion

A variety of molecules have been demonstrated to play important roles in colonization of the early metastatic niche through their systemic secretion and by interacting with recruited

CD11b$^+$ leukocytes (14–19). The identification of direct interactions between these leukocytes and tumor cells within the blood vessels and colonized tissues suggests a role for a conserved adhesion receptor-ligand axis during metastatic progression. Here, we identify galectin-3 as a novel regulator of lung adenocarcinoma metastasis through its presentation within the metastatic niche and binding to the oncofetal disaccharide known as the T-Antigen (Fig. 7). Based on our findings, we propose that early in tumorigenesis, tumors secrete soluble factors, such as IL-6, that induce the mobilization of CD11b$^+$galectin-3$^+$ BMDCs into circulation. Additionally, galectin-3 is presented on macrophages in the early metastatic niche of tumor-bearing mice. As tumors gain metastatic potential, they increase their presentation of the T-Antigen on their surfaces. In the context of our lung adenocarcinoma mouse model, we show that this elevated presentation does not result from increased *O*-glycosylation through core 1 glycosyltransferases, but rather is due to the abrogation of core 1 chain extension conferred by downregulation of C2GnT2 and capping of the motif by the α2-6 sialyltransferase St6GalNAcIV. These changes in transferase activity and T-Antigen presentation result in increased carbohydrate-dependent binding of the tumor cells to galectin-3 and increased metastasis *in vivo*. As the presence of tumors induces elevated numbers of galectin-3$^+$ myeloid cells in the circulation and metastatic niche, these alterations in transferase activity within the tumor cells may represent an essential mechanism by which metastatic cells interact with these pro-tumorigenic leukocytes at those sites. Furthermore, perturbations in expression of these transferases are correlated with humans with NSCLC (Fig. 5 and Supplementary Fig. 13B), and the T-Antigen is frequently overexpressed on many cancers (36), suggesting that this model of glycan regulation may extend to many clinical settings.

Dissemination of tumor cells is thought to occur early in tumorigenesis (39). Recent evidence supports the concept that the rate-limiting step in the formation of clinically-relevant tumors is the adaptation of disseminated cancer cells to their local microenvironments in a manner that permits colonization (11). Additional studies have suggested that early, or even “pre-”, metastatic niches may exist wherein a protumorigenic microenvironment is generated (12). Such microenvironments harbor inflammatory leukocytes that act to promote metastatic colonization (11, 13, 40). Our findings on the mobilization and recruitment of these inflammatory populations by nonmetastatic primary tumors are consistent with the hypothesis that involvement of pro-metastatic stromal populations is, at least in-part, an early event. Thus, adaptations by the metastatic tumor cells that potentiate interactions with these leukocytes may represent the rate-limiting events permitting colonization. Here, we find that alterations in glycosylation that result in T-Antigen presentation is one such event in that it occurs later in tumor progression and promotes interactions with galectin-3 in the metastatic niche.

A variety of studies have implicated galectin-3 in tumor progression and metastasis (1). The majority of these studies have demonstrated strong clinical correlations with advanced stage disease or decreased survival with elevated levels of galectin-3 (4, 5). In agreement with these clinical reports, our model also demonstrated elevated serum levels of galectin-3 in mice bearing tumors (Supplementary Fig. 18). Experimental studies have primarily investigated the roles of galectins in modulating the immune system (3) or in interactions

with blood vessels. In addition to its reported role in promoting angiogenesis (41), surface expression of galectin-3 on endothelial cells has been suggested to promote adhesion of breast and prostate cancer cells to the endothelium through carbohydrate interactions (7). Here, we suggest an additional role for galectin-3 in metastasis in that it is presented within the early metastatic niche on recruited metastasis-associated myeloid cells. Thus, galectin-3 may not act only to promote adhesion to endothelium, but also to promote interactions between the cancer cells and BMDCs within the tissues or within circulation in a manner that not only promotes extravasation but also colonization.

An abundance of clinical and experimental evidence has suggested a role for interleukin 6 (IL-6) in cancer metastasis (19, 21, 42–44). Tumor-derived soluble factors, including a variety of ECM molecules such as laminins and versican (19), have been reported to act upon macrophages, through Toll-like receptors (TLRs), to induce the production of IL-6. Here, we find that lung tumors, themselves, produce IL-6 independent of the presence of the myeloid cells. Our conditioned medium experiments suggest that soluble factors such as IL-6 are capable of inducing the rapid mobilization of $CD11b^{+}Ly6C^{hi}$ and $CD11b^{+}Gr\text{-}1^{+}$ myeloid cells into circulation, which are thought to promote metastasis. Other molecules traditionally considered to be produced by myeloid cells, such as CCL2, can be produced by tumor cells to induce the recruitment of pro-metastatic $CD11b^{+}$ populations (25). The production of cytokines, such as IL-6, by tumors represents another means by which tumors can indirectly promote the development of inflammatory microenvironments at distant sites.

Alterations in glycosylation have long been associated with malignancy (45–47). Many clinical biomarkers are carbohydrate antigens such as CA19-9, CA125, DUPAN-II, and AFP-L3 (48). Furthermore, overexpression of many *O*-linked glycoproteins, such as MUC1, have been correlated with malignancy (49). As a result, this glycoprotein has been the subject of numerous vaccine development initiatives, and these vaccines are typically more efficacious when the glycosylated antigen is used (49, 50). In addition to expression of particular glycoproteins, aberrant glycosyltransferase activity is frequently observed in a variety of cancers. We show that upregulation of St6GalNAcIV and downregulation C2GnT2 preserve presentation of the T-Antigen through prevention of *O*-glycan chain elongation. Together with previous findings of overexpression of *ST6GALNAC5* in breast cancer metastasis to the brain (24) and general increases in sialylation on metastatic cell lines(51), our study suggests a conserved mechanism by which the T-Antigen is presented on metastasizing cells that appears to potentiate colonization through interactions with galectins in the metastatic niche. It is worth noting that a recent study found that another sialyltransferase, ST6GalNAcII, may influence metastatic potential (52). In this case, however, knockdown of ST6GalNAcII in a breast cancer cell line led to an increase in metastasis. While, on the surface, this finding appears to contradict those presented within this manuscript, the data are consistent in that in both cases, glycosylation-dependent galectin-3 binding promotes metastasis formation. One possibility is that the inverse regulation of the two transferases may result in the same functional phenotype, with ST6GalNAcII preventing presentation of the galectin-3 ligand N-Acetyllactosamine or similar ligands, and ST6GalNAcIV promoting expression of the T-Antigen. Previously, we found that the integrin $\alpha 3\beta 1$ promotes metastasis through binding to combinations of

fibronectin with either galectin-3 or -8 (30). Integrins contain a variety of glycosylation sites, and these data may suggest that glycosylation of integrins could promote metastasis through synergistic interactions between galectins and other ECM molecules within the metastatic niche. Regardless of the particular proteins exhibiting these glycosylation patterns, our observations of alterations in transferase expression and T-Antigen presentation in humans with the disease suggests a role for a highly conserved mechanism of glycan-mediated lung cancer metastasis that warrants consideration for therapeutic intervention.

Methods

Cell Lines and Mouse Transplantation Assays

Murine cell lines (a gift from Tyler Jacks and Monte Winslow, Massachusetts Institute of Technology, Cambridge, MA) were described previously (28) and were cultured in DMEM with 10% (vol/vol) fetal bovine serum and 1% L-glutamine. The cell lines were used within five passages of the distributed vials and were tested frequently for consistency in gene expression by qRT-PCR. No additional authentication was performed. All cell lines were tested for pathogens by PCR by the MIT Division of Comparative Medicine during the time period in which they were being used. The human NSCLC lines were provided by the National Cancer Institute (NCI) through the Division of Cancer Treatment and Diagnosis (DCTD) Tumor Repository. The repository authenticates the lines and tests all cell lines for pathogens by PCR prior to distribution. Experiments were performed within five passages of the distributed vials.

All animal procedures were performed in accordance with the MIT Institutional Animal Care and Use Committee under protocol 0211-014-14. Cell injection studies were performed in female B6129SF1/J mice 6–10 weeks of age (Jackson Laboratory, Stock Number 101043). Additionally, IL-6 experiments were performed in B6.129X1(Cg)-Csf3r^{tm1Link}/J and B6.Cg-Lgals3^{tm1Poi}/J mice (Jackson Laboratory, Stock Numbers 017838 and 006338) with C57BL/6J mice as controls (Jackson Laboratory, Stock Number 000664). For CD11b mobilization experiments, mice were injected with 3×10^5 cells resuspended in 100μL of PBS into the subcutaneous region of flanks of mice, while anesthetized with isofluorane. Tumors and peripheral blood were harvested 5–8 weeks following injections. Approximately 1mL of peripheral blood was harvested by cardiac puncture, while mice were anesthetized with isofluorane and used for analysis by flow cytometry. Mice were immediately euthanized following recovery of the blood and their tumors were harvested.

Intrasplenic transplantation assays were performed as previously described(30). Briefly, 5×10^5 cells were resuspended in 100μL of phosphate buffered saline (PBS). Animals were anesthetized with 2.5% isofluorane and administered buprenorphine (150μg/kg). Fur was removed with surgical clippers and the incision site was sterilized with Betadine and 70% ethanol. The spleen was exposed through a small incision and cells were injected into the tip of the spleen with a 27-gauge needle. The cells were allowed to travel through circulation for two minutes prior to removal of the spleen. The splenic vessels were then cauterized and the entire spleen was removed. The muscle wall was closed with 5-0 dissolvable sutures, and the skin was closed with 7mm wound clips (Roboz). Mice were euthanized two weeks following injection, and their livers were excised. GFP$^+$ tumors were visualized and

quantified using an epifluorescence dissection scope (Nikon). Tissues were fixed in 4% paraformaldehyde and stained with hematoxylin and eosin following paraffin embedding.

Immunohistochemical and Immunocytochemical Analysis

Following necropsy, tumors and livers were fixed overnight in 4% paraformaldehyde at 4°C. Tissues used for paraffin embedding were transferred to cassettes and placed in 70% ethanol. Those used for frozen sections were placed in 30% sucrose overnight at 4°C. Tissues were then transferred to O.C.T. compound (Tissue-Tek) for 4 hours at room temperature followed by freezing in isopentane (Sigma) placed in a liquid nitrogen bath. Co-staining of galectin-3 and F4/80 was performed on frozen sections using antibody clones M3/38 (BioLegend) and CI:A3-1 (BioLegend), respectively. Nuclei were stained with Hoechst (Invitrogen). For studies of livers prior to the detection of overt metastases, excised tissues were examined grossly for the appearance of nodules and microscopically, following staining, for the presence of tumors.

For fluorescent lectin analysis of T-Antigen presentation, cells were stained with PNA-AlexaFluor 647 (invitrogen). All paraffin sections were developed using DAB and counterstained with hematoxylin. Carbo-Free Blocking Solution (Vector Laboratories) was used for all staining involving the use of peanut agglutinin. Endogenous peroxidase activity was blocked using the Dual Endogenous Enzyme Block (Dako). PNA staining of human tissue microarrays was performed with PNA-HRP (Sigma, 4μg/mL) following antigen retrieval in citrate buffer. Staining of the Human Lung Cancer and Normal Tissue Microarray (US Biomax, Inc) was scored for the presence of surface T-Antigen staining in a blinded fashion.

All images were acquired using an inverted Nikon Ti-E epifluorescence microscope using Elements software (Nikon). Pseudocoloring was performed using Elements or ImageJ (NIH). Quantification of histology was performed using Elements.

Western and PNA Lectin Blot Analysis

Cell lysates were harvested in RIPA buffer (Sigma) containing Complete Protease Inhibitor (Roche) and Phospho Stop (Roche) on ice and run on SDS-PAGE gels. PVDF membranes were stained for galectin-3 (Abcam, ab53082, 1:500, or BioLegend, M3/38, 1:1000), galectin-8 (Abcam, ab69631, 1:500), and α-tubulin (Cell Signaling, 2125, 1:1000). Lectin blotting for glycans was performed using PNA-Biotin (Sigma) followed by detection using the ABC Elite Kit (Vector Labs, PK-6100) or PNA-Peroxidase conjugates (Sigma). Ponceau S solution (Thermo) was used for total protein detection following transfer to PVDF membranes.

For liver homogenate western blots, mice bearing 393M1 flank tumors or no tumors were perfused by intracardiac injection of 20mL of phosphate buffered saline. Livers were then excised and 50mg portions were added to gentleMACS M tubes (Miltenyi Biotech) in 4.5mL of RIPA (Sigma) with Complete Protease Inhibitors (Roche). Tissue was dissociated using the gentleMACS Octo Dissociator (Miltenyi Biotech) and run on polyacrylamide gels as described above.

Galectin-3 ELISA

Peripheral blood was harvested from mice without tumors or bearing contralateral flank tumors of both 802T4 and 393T5 cell lines by cardiac puncture as described above. Blood was collected in serum collection tubes (Capiject) and allowed to clot for 30 minutes prior to centrifugation and removal of serum. The galectin-3 ELISA kit (R&D Systems) was used according to the manufacturer's instructions.

Cell Surface Protein Isolation

Cell surface proteins were isolated prior to Western blot analysis using Thermo Scientific kit 89881 following the manufacturer's instructions. Briefly, cells are washed followed by biotinylation of the surface proteins by a Sulfo-NHS-Biotin through conjugation to free amines. The reaction is quenched and cells are harvested and lysed. Lysate is washed through a column containing a neutravidin resin to capture the biotinylated surface proteins. Finally, the disulfide linkage is reduced through incubation with 50mM DTT and the proteins are captured.

Flow Cytometric Analysis

Peripheral blood was drawn by cardiac puncture and transferred to K2 EDTA 5.4mg Plus Blood Collection Tubes (BD Vacutainer, BD Biosciences). Red blood cells were lysed using RBC lysis buffer (eBiosciences). Cells were fixed in 4% paraformaldehyde and washed prior to staining. Cells were blocked using anti-mouse CD16/CD32 antibody clone 2.4G2 (BD Biosciences). Antibodies against mouse antigens were: CD11b (M1/70, BD Biosciences), CD115 (AFS98, eBiosciences), Mac-2 (M3/38, BioLegend), Ly-6C (HK1.4, BioLegend), and Gr-1 (RB6-8C6, BioLegend). Flow cytometry was performed on a LSR Fortessa (BD Biosciences) and analyzed using Flowjo (Tree Star).

Magnetic separation of $CD11b^+$ cells was performed using CD11b MACS microbeads (Miltenyi). Following collection of peripheral blood by cardiac puncture and lysis of erythrocytes, cells were incubated with the MACS beads following the manufacturer's instructions. $CD11b^+$ cells were isolated using MACS MS Collection Columns (Miltenyi).

Peanut agglutinin staining was performed by incubating 3×10^5 cells in PBS with 10μL PNA-AlexaFluor 647 (invitrogen) on ice for 30 minutes. Fluorescent galectin-3 was produced by reacting recombinant murine galectin-3 (R&D Systems) with DyLight 650 NHS Ester (Thermo Pierce). Conjugated protein was purified by FPLC and concentrated to 0.5mg/mL using 3,000 MWCO Amicon centrifugal filter units (Millipore). Cells were stained by incubating 3×10^5 cells in PBS with 10μL of the fluorescent galectin-3 on ice for 30 minutes.

For galectin-3 binding inhibition experiments on tumor cells, cells were incubated with galectin-3, as described above in the presence of 20mM *N*-Acetyl-D-lactosamine (Carbosynth) or sucrose (Sigma). For competition of galectin-3 presentation on leukocytes, peripheral blood was harvested from mice bearing 393M1 flank tumors, as described above. Cells were incubated with 200mM β-lactose (Sigma) or sucrose (Sigma) in 2% FBS for 30 minutes on ice. Cells were then fixed, stained, and analyzed by flow cytometry.

Conditioned Media Experiments

Twenty-five milliliters of conditioned medium was harvested from one T150 flask of 393M1s following three days of culture. This medium (or fresh control medium with serum) was filtered through 0.2μm filters and concentrated 15-fold using 3,000 MWCO centrifugal filters (Amicon). 200μL of medium was injected into the lateral tail vein of mice. Two hours after injections, peripheral blood was harvested from the mice by cardiac puncture, as described above, followed by fixation, staining, and flow cytometric analysis. For experiments involving recombinant galectin-3, murine recombinant galectin-3 (R&D Systems) was supplemented to the medium at 1μg per injection. For IL-6 experiments, murine recombinant IL-6 (R&D Systems) was supplemented to the medium at 50ng per injection.

Luminex Cytokine Profiling

Cytokine profiles of 100uL cell culture supernatant from control and conditioned media were assessed using a EMD Millipore Milliplex custom magnetic bead panel using manufacturer's protocol: IL-2, IFNg, IL-10, TNFa, IL-17a, IL-4, IL-5, IL-6. Luminex assays were analyzed using Bioplex 200 with Bioplex Manager 6.1.

RNA Isolation and Expression Profiling

Murine gene expression microarray analysis was described previously(28, 30) and is available from NCBI under accession number GSE40222 and GSE26874. Human NSCLC expression microarray data was accessed from NCBI accession number GSE32474. RNA was isolated using RNeasy mini kits (Qiagen) according to the manufacturer's instructions. cDNA reactions were performed using iScript cDNA synthesis kit (Bio-Rad). qPCR reactions were performed using 2μL of cDNA, 12.5μL of IQ SYBR Green Supermix (Bio-Rad), and 1μmol of each primer. Fold change is reported following analysis using the $\Delta\Delta C_t$ method where genes were normalized to *Hprt* housekeeping control. Primers were: *St6galnac4* forward 5′-GGTTGGTTCACCATGATTCTG-3′, *St6galnac4* reverse 5′-GGAGCGGGGACTCTTCTC-3′, *Gcnt3* forward 5′-GCAGCCAAGAAGGTACCAAA-3′, *Gcnt3* reverse 5′-ACAGGCGAGGACCATCAA-3′ or forward 5′-ATGAGAGCCATTGCGAGACT-3′ reverse 5′-CTTGTTGGCCAAGAGGTGAT-3′, *Hprt* forward 5′-GTCAACGGGGGACATAAAAG-3′, *Hprt* reverse 5′-CAACAATCAAGACATTCTTTACA-3′. Gene expression analysis and visualizations were performed using Spotfire (Tibco) and MATLAB (Mathworks).

Human Copy Number Analysis

Copy number determinations of *GCNT3* and *IL6* were performed using Oncomine (53) based on publicly-available data from the Cancer Genome Atlas (54).

Hairpins and Plasmids

Knockdown of St6galnac4 was performed using short-hairpin RNA (5′-TTCTGCTCCTCACACTGTGCATCTTGACA-3′) or a control hairpin targeting firefly luciferase in the pGFP-V-RS vector (Origene, TG502032 and TR30002). Plasmids were packaged into retroviruses using the Phoenix-Eco system. Viral supernatant was filtered

using 0.45μm syringe filters and cultured with 393M1 cells at no dilution. Transduced cells were selected with puromycin (Invitrogen), and knockdown efficiency was determined by qRT-PCR following four weeks of culture. Tansfection of *Gcnt3* was performed using Lipofectamine (Invitrogen) according to the manufacturer's instructions with plasmids purchased from Origene (MC215765). Knockdown of Lgals3 was performed using two short-hairpin RNAs (Sigma, shGal3-3: 5′-CCGGGCAGTACAACCATCGGATGAACTCGAGTTCATCCGATGGTTGTACTGCTTTTT G-3′; shGal3-5: 5′-CCGGCCGCATGCTGATCACAATCATCTCGAGATGATTGTGATCAGCATGCGGTTTTT G-3′) or a control hairpin targeting firefly luciferase in (Sigma, SHC007V). Additionally, a second hairpin system was used to knockdown *St6galnac4* from Sigma (shSt6galnac4-2: CCGGGTACACCTTCACTGAACGCATCTCGAGATGCGTTCAGTGAAGGTGTACTTTTT G).

In vitro Proliferation Assays

Cells expressing hairpins against *St6galnac4* or control hairpins were seeded into 24-well plates. New wells were trypsinized and counted using a hemocytometer with Trypan Blue exclusion at 24 hour intervals.

Supplementary Material

Refer to Web version on PubMed Central for supplementary material.

Acknowledgments

Grant Support

This work was supported in part by the Koch Institute Support (core) Grant P30-CA14051 from the National Cancer Institute. N. Reticker-Flynn is supported by a Ludwig Center for Molecular Oncology Graduate Fellowship. S. Bhatia is an HHMI investigator. This work was supported by a Stand Up To Cancer Dream Team Translational Research Grant, Grant Number SU2C-AACR-DT0309 (Stand Up To Cancer is a program of the Entertainment Industry Foundation administered by the American Association for Cancer Research), Howard Hughes Medical Institute, and the Koch CTC Project.

The authors thank R. Weinberg and H. Fleming for critical reading of the manuscript. They thank R. Hynes, J. Love, D. Haber, N. Stebbins, C. Sullivan, and all members of the S. Bhatia lab for their insightful discussions. They thank M. Winslow and T. Jacks for providing the cell lines and general insight. They thank the Koch Institute Swanson Biotechnology Center Core Facilities for technical support, specifically with tissue sectioning and usage of flow cytometers. They thank the TCGA and acknowledge use of the TCGA Data Portal. The authors wish to dedicate this manuscript to the memory of Officer Sean Collier for his caring service to the MIT community and for his sacrifice.

References

1. Liu F-T, Rabinovich GA. Galectins as modulators of tumour progression. Nat Rev Cancer. 2005; 5:29–41. [PubMed: 15630413]
2. Almkvist J, Karlsson A. Galectins as inflammatory mediators. Glycoconj J. 2004; 19:575–81. [PubMed: 14758082]
3. Rabinovich GA, Toscano MA. Turning 'sweet' on immunity: galectin-glycan interactions in immune tolerance and inflammation. Nat Rev Immunol. 2009; 9:338–52. [PubMed: 19365409]

4. Iurisci I, Tinari N, Natoli C, Angelucci D, Cianchetti E, Iacobelli S. Concentrations of Galectin-3 in the Sera of Normal Controls and Cancer Patients. Clinical Cancer Research. 2000; 6:1389–93. [PubMed: 10778968]
5. Balan V, Nangia-Makker P, Raz A. Galectins as Cancer Biomarkers. Cancers. 2010; 2:592–610. [PubMed: 23658855]
6. John CM, Leffler H, Kahl-Knutsson B, Svensson I, Jarvis GA. Truncated Galectin-3 Inhibits Tumor Growth and Metastasis in Orthotopic Nude Mouse Model of Human Breast Cancer. Clinical Cancer Research. 2003; 9:2374–83. [PubMed: 12796408]
7. Glinsky VV, Glinsky GV, Rittenhouse-Olson K, Huflejt ME, Glinskii OV, Deutscher SL, et al. The Role of Thomsen-Friedenreich Antigen in Adhesion of Human Breast and Prostate Cancer Cells to the Endothelium. Cancer Research. 2001; 61:4851–7. [PubMed: 11406562]
8. Bian CF, Zhang Y, Sun H, Li DF, Wang DC. Structural basis for distinct binding properties of the human galectins to Thomsen-Friedenreich antigen. PLoS ONE. 2011; 6:e25007. [PubMed: 21949831]
9. Yu L-G. The oncofetal Thomsen–Friedenreich carbohydrate antigen in cancer progression. Glycoconjugate Journal. 2007; 24:411–20. [PubMed: 17457671]
10. Springer GF. Immunoreactive T and Tn epitopes in cancer diagnosis, prognosis, and immunotherapy. J Mol Med (Berl). 1997; 75:594–602. [PubMed: 9297627]
11. Joyce JA, Pollard JW. Microenvironmental regulation of metastasis. Nat Rev Cancer. 2009; 9:239–52. [PubMed: 19279573]
12. Psaila B, Lyden D. The metastatic niche: adapting the foreign soil. Nat Rev Cancer. 2009; 9:285–93. [PubMed: 19308068]
13. Pollard JW. Tumour-educated macrophages promote tumour progression and metastasis. Nat Rev Cancer. 2004; 4:71–8. [PubMed: 14708027]
14. Kaplan RN, Riba RD, Zacharoulis S, Bramley AH, Vincent L, Costa C, et al. VEGFR1-positive haematopoietic bone marrow progenitors initiate the pre-metastatic niche. Nature. 2005; 438:820–7. [PubMed: 16341007]
15. Erler JT, Bennewith KL, Cox TR, Lang G, Bird D, Koong A, et al. Hypoxia-Induced Lysyl Oxidase Is a Critical Mediator of Bone Marrow Cell Recruitment to Form the Premetastatic Niche. Cancer Cell. 2009; 15:35–44. [PubMed: 19111879]
16. Oskarsson T, Acharyya S, Zhang XHF, Vanharanta S, Tavazoie SF, Morris PG, et al. Breast cancer cells produce tenascin C as a metastatic niche component to colonize the lungs. Nat Med. 2011; 17:867–74. [PubMed: 21706029]
17. McAllister SS, Gifford AM, Greiner AL, Kelleher SP, Saelzler MP, Ince TA, et al. Systemic Endocrine Instigation of Indolent Tumor Growth Requires Osteopontin. Cell. 2008; 133:994–1005. [PubMed: 18555776]
18. Malanchi I, Santamaria-Martinez A, Susanto E, Peng H, Lehr H-A, Delaloye J-F, et al. Interactions between cancer stem cells and their niche govern metastatic colonization. Nature. 2012; 481:85–9. [PubMed: 22158103]
19. Kim S, Takahashi H, Lin W-W, Descargues P, Grivennikov S, Kim Y, et al. Carcinoma-produced factors activate myeloid cells through TLR2 to stimulate metastasis. Nature. 2009; 457:102–6. [PubMed: 19122641]
20. Du R, Lu KV, Petritsch C, Liu P, Ganss R, Passegué E, et al. HIF1α Induces the Recruitment of Bone Marrow-Derived Vascular Modulatory Cells to Regulate Tumor Angiogenesis and Invasion. Cancer Cell. 2008; 13:206–20. [PubMed: 18328425]
21. Kim M-Y, Oskarsson T, Acharyya S, Nguyen DX, Zhang XHF, Norton L, et al. Tumor Self-Seeding by Circulating Cancer Cells. Cell. 2009; 139:1315–26. [PubMed: 20064377]
22. Kang Y, Siegel PM, Shu W, Drobnjak M, Kakonen SM, Cordón-Cardo C, et al. A multigenic program mediating breast cancer metastasis to bone. Cancer Cell. 2003; 3:537–49. [PubMed: 12842083]
23. Minn AJ, Gupta GP, Siegel PM, Bos PD, Shu W, Giri DD, et al. Genes that mediate breast cancer metastasis to lung. Nature. 2005; 436:518–24. [PubMed: 16049480]
24. Bos PD, Zhang XHF, Nadal C, Shu W, Gomis RR, Nguyen DX, et al. Genes that mediate breast cancer metastasis to the brain. Nature. 2009; 459:1005–9. [PubMed: 19421193]

25. Qian B-Z, Li J, Zhang H, Kitamura T, Zhang J, Campion LR, et al. CCL2 recruits inflammatory monocytes to facilitate breast-tumour metastasis. Nature. 2011; 475:222–5. [PubMed: 21654748]
26. Yang L, Huang J, Ren X, Gorska AE, Chytil A, Aakre M, et al. Abrogation of TGF beta signaling in mammary carcinomas recruits Gr-1+CD11b+ myeloid cells that promote metastasis. Cancer Cell. 2008; 13:23–35. [PubMed: 18167337]
27. Jackson EL, Willis N, Mercer K, Bronson RT, Crowley D, Montoya R, et al. Analysis of lung tumor initiation and progression using conditional expression of oncogenic K-ras. Genes & Development. 2001; 15:3243–8. [PubMed: 11751630]
28. Winslow MM, Dayton TL, Verhaak RGW, Kim-Kiselak C, Snyder EL, Feldser DM, et al. Suppression of lung adenocarcinoma progression by Nkx2-1. Nature. 2011; 473:101–4. [PubMed: 21471965]
29. DuPage M, Cheung AF, Mazumdar C, Winslow MM, Bronson R, Schmidt LM, et al. Endogenous T Cell Responses to Antigens Expressed in Lung Adenocarcinomas Delay Malignant Tumor Progression. Cancer Cell. 2011; 19:72–85. [PubMed: 21251614]
30. Reticker-Flynn NE, Malta DFB, Winslow MM, Lamar JM, Xu MJ, Underhill GH, et al. A combinatorial extracellular matrix platform identifies cell-extracellular matrix interactions that correlate with metastasis. Nat Commun. 2012; 3:1122. [PubMed: 23047680]
31. Dong S, Hughes RC. Macrophage surface glycoproteins binding to galectin-3 (Mac-2-antigen). Glycoconj J. 1997; 14:267–74. [PubMed: 9111144]
32. Hiratsuka S, Watanabe A, Aburatani H, Maru Y. Tumour-mediated upregulation of chemoattractants and recruitment of myeloid cells predetermines lung metastasis. Nat Cell Biol. 2006; 8:1369–75. [PubMed: 17128264]
33. Sano H. Human galectin-3 is a novel chemoattractant for monocytes and macrophages. J Immunol. 2000; 165:2156–64. [PubMed: 10925302]
34. Sato S, Ouellet N, Pelletier I, Simard M, Rancourt A, Bergeron MG. Role of galectin-3 as an adhesion molecule for neutrophil extravasation during streptococcal pneumonia. J Immunol. 2002; 168:1813–22. [PubMed: 11823514]
35. Functional Glycomics Gateway; Consortium for Functional Glycomics. 2010. http://www.functionalglycomics.org/
36. Springer GF. T and Tn, general carcinoma autoantigens. Science. 1984; 224:1198–206. [PubMed: 6729450]
37. Hsu Y-C, Yuan S, Chen H-Y, Yu S-L, Liu C-H, Hsu P-Y, et al. A Four-Gene Signature from NCI-60 Cell Line for Survival Prediction in Non–Small Cell Lung Cancer. Clinical Cancer Research. 2009; 15:7309–15. [PubMed: 19920108]
38. Inka B. Pathways of O-glycan biosynthesis in cancer cells. Biochimica et Biophysica Acta (BBA) - General Subjects. 1999; 1473:67–95.
39. Hüsemann Y, Geigl JB, Schubert F, Musiani P, Meyer M, Burghart E, et al. Systemic Spread Is an Early Step in Breast Cancer. Cancer Cell. 2008; 13:58–68. [PubMed: 18167340]
40. Coussens LM, Werb Z. Inflammation and cancer. Nature. 2002; 420:860–7. [PubMed: 12490959]
41. Nangia-Makker P. Galectin-3 induces endothetial cell morphogenesis and angiogenesis. Am J Pathol. 2000; 156:899–909. [PubMed: 10702407]
42. Ueda T, Shimada E, Urakawa T. Serum levels of cytokines in patients with colorectal cancer: Possible involvement of interleukin-6 and interleukin-8 in hematogenous metastasis. J Gastroenterol. 1994; 29:423–9. [PubMed: 7951851]
43. Blay J-Y, Negrier S, Combaret V, Attali S, Goillot E, Merrouche Y, et al. Serum Level of Interleukin 6 as a Prognosis Factor in Metastatic Renal Cell Carcinoma. Cancer Research. 1992; 52:3317–22. [PubMed: 1596890]
44. Nakashima J, Tachibana M, Horiguchi Y, Oya M, Ohigashi T, Asakura H, et al. Serum Interleukin 6 as a Prognostic Factor in Patients with Prostate Cancer. Clinical Cancer Research. 2000; 6:2702–6. [PubMed: 10914713]
45. Burger MM. Surface changes in transformed cells detected by lectins. Fed Proc. 1973; 32:91–101. [PubMed: 4346328]
46. Kim Y, Varki A. Perspectives on the significance of altered glycosylation of glycoproteins in cancer. Glycoconjugate Journal. 1997; 14:569–76. [PubMed: 9298689]

47. Hakomori S. Glycosylation defining cancer malignancy: New wine in an old bottle. Proceedings of the National Academy of Sciences. 2002; 99:10231–3.

48. Ueda K. Glycoproteomic strategies: From discovery to clinical application of cancer carbohydrate biomarkers. PROTEOMICS – Clinical Applications. 2013; 7:607–17.

49. Kufe DW. Mucins in cancer: function, prognosis and therapy. Nat Rev Cancer. 2009; 9:874–85. [PubMed: 19935676]

50. Lakshminarayanan V, Thompson P, Wolfert MA, Buskas T, Bradley JM, Pathangey LB, et al. Immune recognition of tumor-associated mucin MUC1 is achieved by a fully synthetic aberrantly glycosylated MUC1 tripartite vaccine. Proc Natl Acad Sci U S A. 2012; 109:261–6. [PubMed: 22171012]

51. Yogeeswaran G, Salk PL. Metastatic potential is positively correlated with cell surface sialylation of cultured murine tumor cell lines. Science. 1981; 212:1514–6. [PubMed: 7233237]

52. Murugaesu N, Iravani M, van Weverwijk A, Ivetic A, Johnson DA, Antonopoulos A, et al. An In Vivo Functional Screen Identifies ST6GalNAc2 Sialyltransferase as a Breast Cancer Metastasis Suppressor. Cancer Discovery. 2014; 4:304–17. [PubMed: 24520024]

53. Rhodes DR, Yu J, Shanker K, Deshpande N, Varambally R, Ghosh D, et al. ONCOMINE: a cancer microarray database and integrated data-mining platform. Neoplasia. 2004; 6:1–6. [PubMed: 15068665]

54. The Cancer Genome Atlas. https://tcga-data.nci.nih.gov/tcga/tcgaHome2.jsp

Significance

While clinical observations of elevated serum galectin-3 levels and altered glycosylation have been associated with malignancy, we identify novel roles for glycosyltransferases in promoting adhesion to galectins in the metastatic niche. This identification of a cytokine-leukocyte-glycosylation axis in metastasis provides mechanistic explanations for clinical associations between malignancy and aberrant glycosylation.

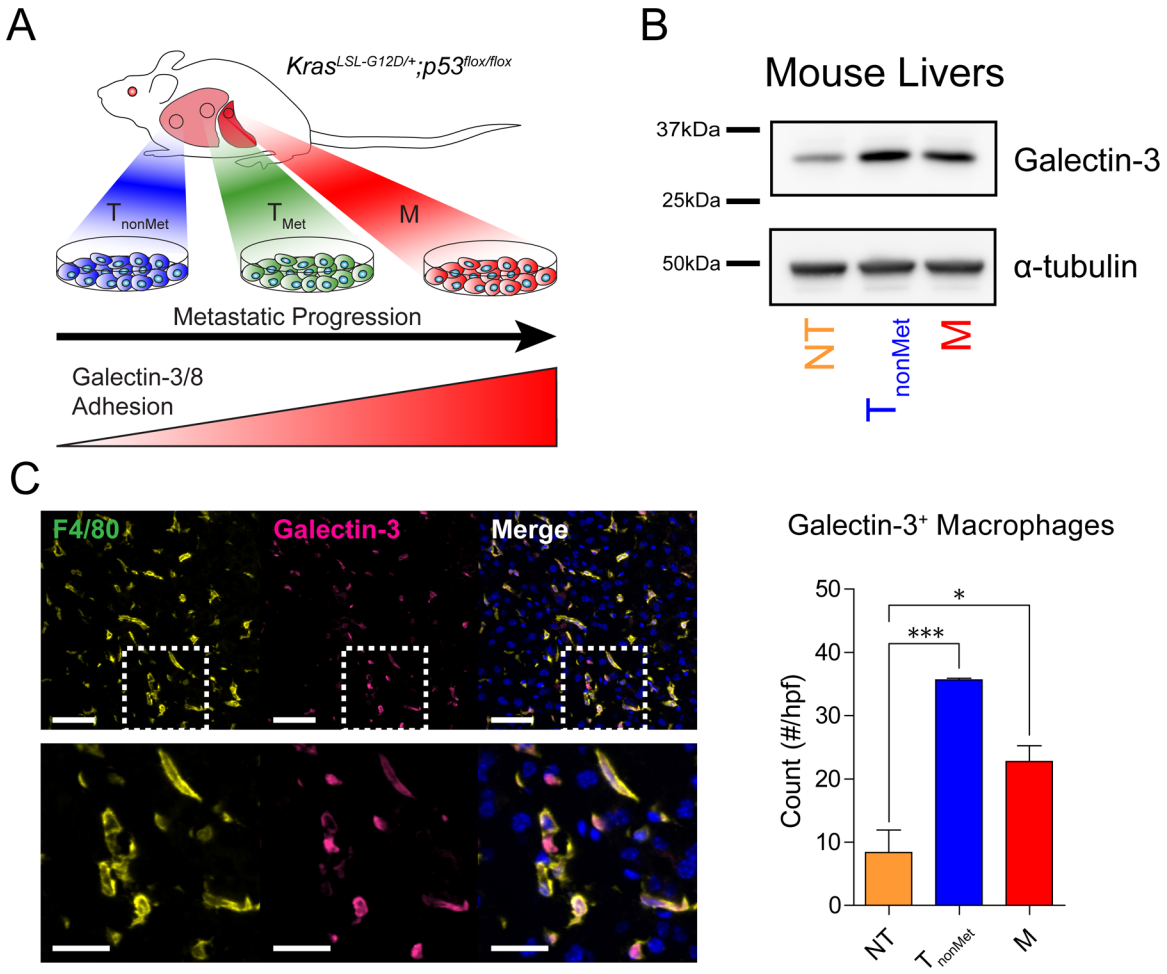

Figure 1. Mice bearing tumors have accumulation of the adhesion ligand, galectin-3, in the early metastatic niche

(A) Cell lines are generated from autochthonous tumors in *Kras*$^{LSL\text{-}G12D/+}$;*p53*$^{flox/flox}$ mice following tumor development. The lines, which represent discrete stages of metastasis, are derived from primary tumors that did not metastasize (T_{nonMet}), primary tumors that gave rise to metastases (T_{Met}), lymph node metastases (N, not shown), and distant metastases (M). Lines derived from increasingly metastatic tumors exhibit increased adhesion to galectin-3 and galectin-8. (B) Mice bearing the no tumors, T_{nonMet}, and M tumors were analyzed for the presence of galectin-3 in their livers prior to the detection of overt metastases. Mice were perfused with saline prior to homogenization of liver tissue and analysis by western blot. (C) Left: Immunostaining of livers from mice bearing M tumors with no detectable overt metastases in their livers for the presence of macrophages (F4/80, green) and galectin-3 (pink). Nuclei (blue) are stained with Hoechst. Dashed boxes in the top row highlight the area shown in the bottom row. Scale bars in (C) are 50μm (top) and 25μm (bottom). Right: Quantification of galectin-3^{pos}F4/80^{pos} cells in the livers of mice without tumors, T_{nonMet} tumors, or M tumors. Error bars are s.e.m. *P*-values in (C) were determined by One-way ANOVA with Tukey's Multiple Comparison Test. * $P < 0.05$; *** $P < 0.001$.

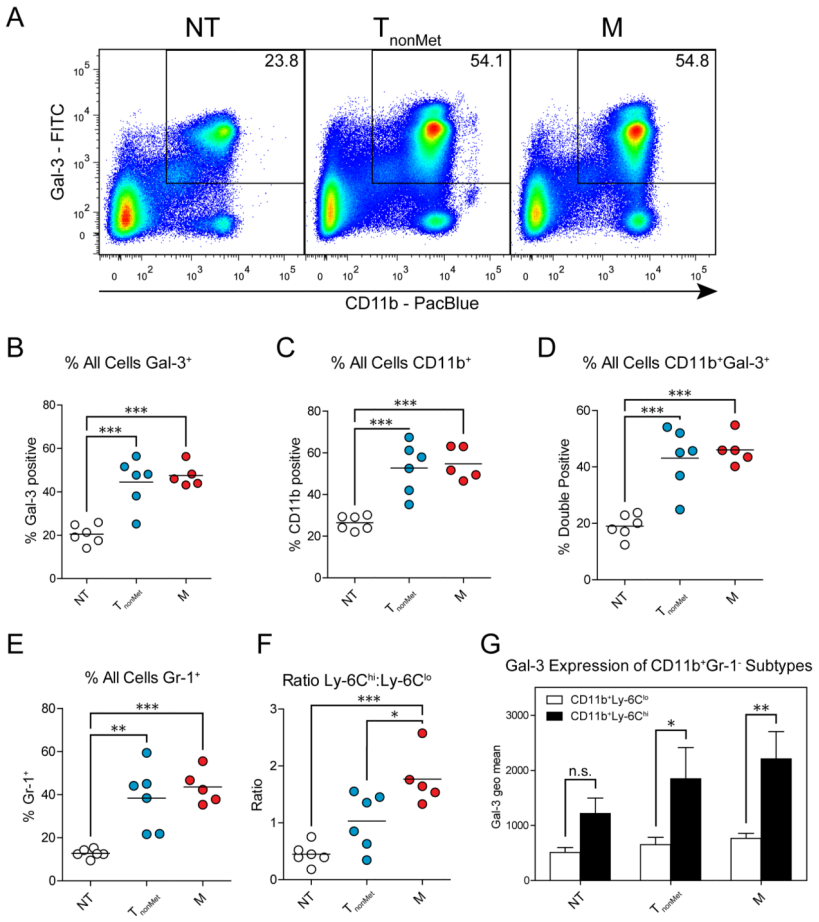

Figure 2. Tumor-derived soluble factors induce the mobilization of galectin-3$^+$ myeloid cells into peripheral circulation early in tumorigenesis

Wild-type mice or mice bearing T_{nonMet} (802T4) or M (393M1) tumors were analyzed for the presence of galectin-3$^+$ leukocytes in their peripheral blood by flow cytometry. (A) Analysis of staining for galectin-3 and CD11b on all leukocytes from mice without tumors (NT), T_{nonMet} tumors, or M tumors. Numbers represent percentages of all leukocytes that were double positive. (B) Percentage of all leukocytes that were galectin-3$^+$. (C) Percentage of all cells that were CD11b$^+$. (D) Percentage of all cells that were CD11b$^+$galectin-3$^+$. (E) Percentage of all leukocytes that were Gr-1$^+$. (F) Ratio of CD11b$^+$Ly-6C^{hi} cells to CD11b$^+$Ly-6C^{lo} cells. (G) Galectin-3 expression on Ly-6C^{lo} and Ly-6C^{hi} cells. *P*-values in (B-F) were determined by One-way ANOVA with Tukey's Multiple Comparison Test. *P*-values in (G) were determined by Two-way ANOVA with Bonferroni post-test. * $P < 0.05$; ** $P < 0.01$; *** $P < 0.001$.

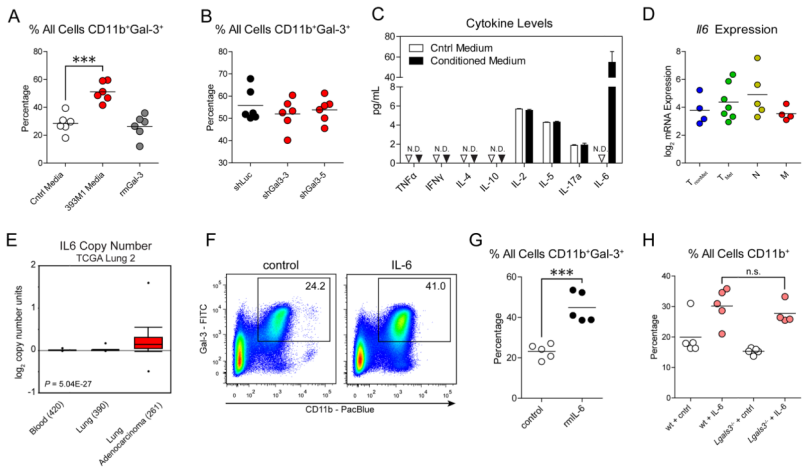

Figure 3. Secretion of IL-6 by tumors induces the rapid mobilization of CD11b$^+$galectin-3$^+$ leukocytes

(A) Analysis of CD11b$^+$galectin-3$^+$ myeloid cell mobilization to peripheral blood following injections of control medium (white), M line conditioned medium (red), or recombinant murine galectin-3 supplemented control medium (gray). (B) Analysis of CD11b$^+$galectin-3$^+$ myeloid cell mobilization following injections of conditioned media from M lines containing either a control hairpin (shLuc, black) or galectin-3 hairpins (red). (C) Luminex cytokine levels of the conditioned medium. (D) Gene expression microarray analysis of *Il6* expression in all cell lines from the four classes. (E) *IL6* exhibits a gain of copy number in human lung adenocarcinomas compared to normal lung tissue or blood ($P = 5.04 \times 10^{-27}$) in the “Lung adenocarcinoma” data set available from The Cancer Genome Atlas website (see Methods). (F,G) Analysis of CD11b$^+$galectin-3$^+$ cell mobilization to peripheral blood following injections of control medium or medium supplemented with recombinant murine IL-6. (H) Mobilization of CD11b$^+$ leukocytes in wild-type and galectin-3 knockout (*Lgals3*$^{-/-}$) mice following IL-6 injections. Error bars in (C) are s.e.m. ‘N.D.’: not detected. *P*-values in (A) and (H) were calculated by One-way ANOVA with Tukey’s Multiple Comparison Test. *P*-value in (G) determined by Student’s t-test. *** $P < 0.001$; ‘n.s.’ not significant.

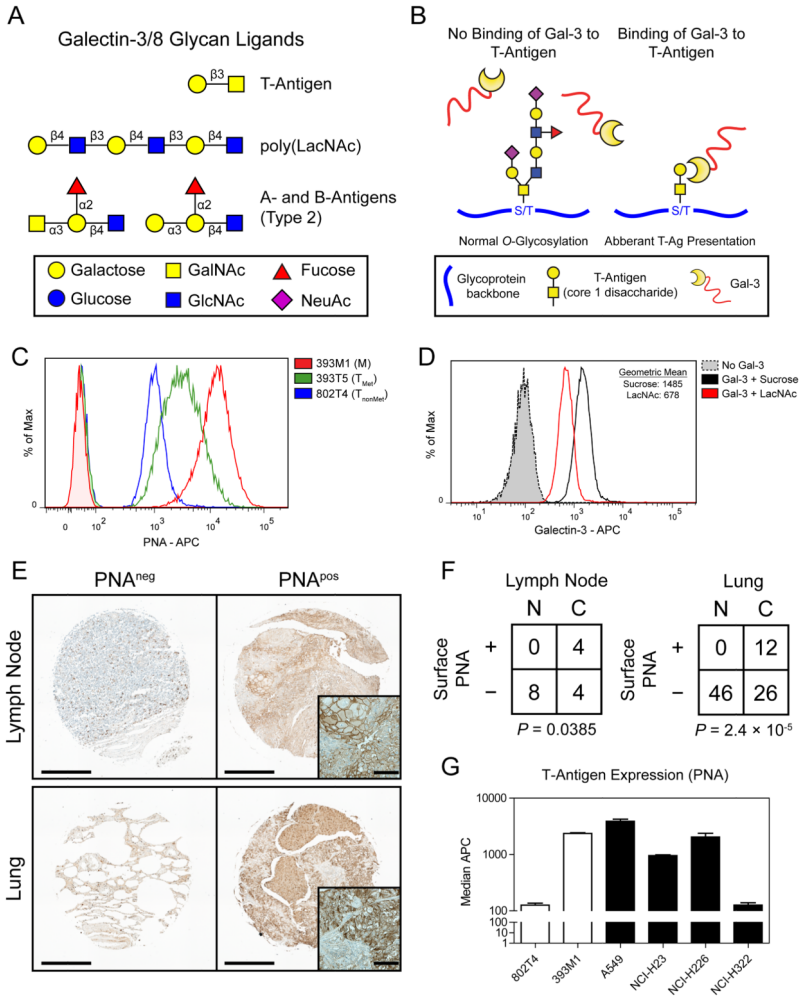

Figure 4. Elevated Thomsen-Friedenreich Antigen presentation promotes increased galectin-3 adhesion in metastatic populations

(A) Potential carbohydrate ligands for the galectin-3 carbohydrate recognition domain (CRD). The T-Antigen (Galβ1-3GalNac-α1-O-S/T) is specific for the CRD of galectin-3 and -8. *N*-Acetyllactosamine (LacNAc) binds the CRD of all galectins and exhibits increased affinities when in a polymeric form. The A- B- Type 2 blood group antigens have reported affinities for a variety of galectins, including galectin-3, by glycan array analysis (35). (B) On normal cells binding of galectin-3 to the T-Antigen on glycoproteins is occluded as the epitope is masked by further glycan extension. On malignant cells, abberant expression of the disaccharide without further glycosylation permits galectin-3 binding. (C) Peanut agglutinin (PNA) labeling of the T-Antigen on representative cell lines from the T_{nonMet} (blue), T_{Met} (green), and M (red) classes as determined by flow cytometry. (D) Binding of galectin-3 fluorophore conjugates in the presence of a glycan competitor for galectin-3, *N*-acetyllactosamine (LacNAc), or control disaccharide (sucrose). (E–F) Human NSCLC tissue microarrays were analyzed for surface T-Antigen presentation by PNA staining. (E) Sample tissue staining in lung and lymph node tissue. Examples of tissues scored as PNA^{neg} and PNA^{pos} are shown. (F) Quantification of TMA spots for PNA staining: ‘N’: non-cancerous tissue; ‘C’: cancer tissue. (G) PNA labeling of human NSCLC cell lines as determined by

flow cytometry. *P*-values in (F) determined by Fisher's Exact Test. Scale bars in (E) are 400μm (100μm for insets).

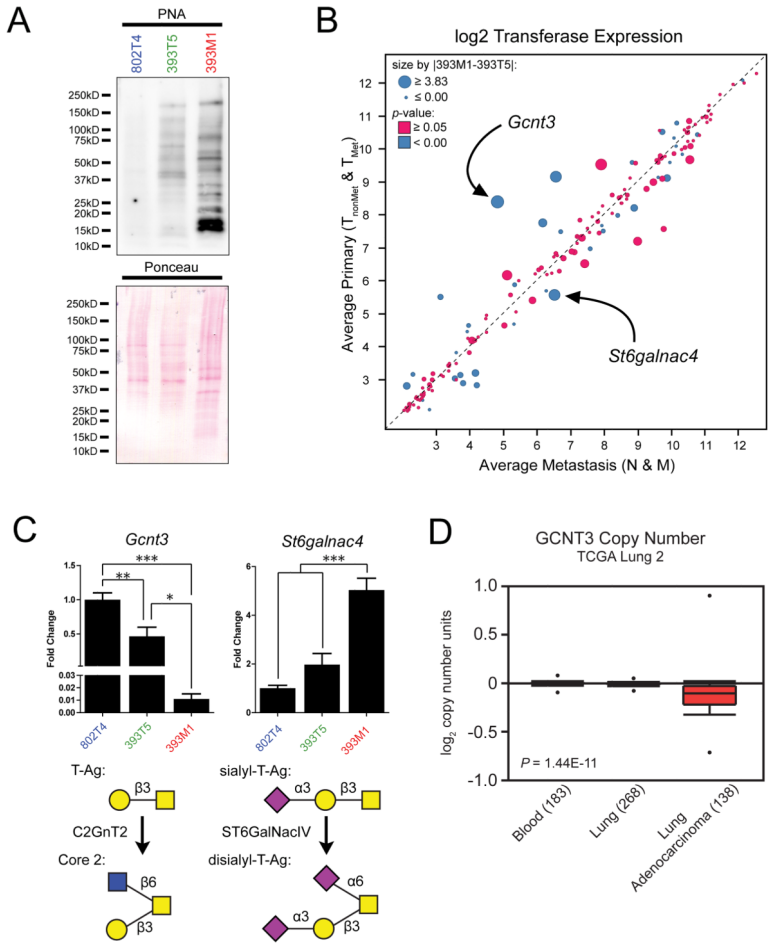

Figure 5. Metastatic cells downregulate*Gcnt3* and upregulate *St6galnac4*

(A) Lectin blot of surface proteins. Cell surface proteins were isolated from representative T_{nonMet} (802T4), T_{Met} (393T5), and M (393M1) lines and run on SDS-PAGE gels. Membranes were blotted for the T-Antigen with PNA. (B) Gene expression microarray analysis of all glycosyltansferases. The average expression for all primary tumor-derived lines (ordinate) is plotted against the average expression for all metastatic lines (abscissa). Size of points represents the absolute difference in expression between the clonally-related T_{Met} and M lines (393T5 and 393M1, respectively). The color represents statistical significance of the differences between any two adjacent cell line classes (i.e. T_{nonMet} vs. T_{Met}, T_{Met} vs. N, N vs. M) as determined by Student's t-test. The dashed line represents equivalent expression between the metastatic and primary tumor-derived lines. (C) qRT-PCR analysis of transferase gene expression. Top: gene expression of *Gcnt3* and *St6galnac4* in representative T_{nonMet}, T_{Met}, and M cell lines. Bottom: C2GnT2 (*Gcnt3*) can transfer a GlcNAc to the core GalNAc of T-Antigen by a β1-6 linkage. St6galnac4 can transfer a NeuAc to the core GalNAc of the sialyl-T-Antigen. (D) *GCNT3* exhibits a loss of copy number in human lung adenocarcinomas compared to normal lung tissue or blood ($P = 1.44 \times 10^{-11}$) in the "Lung adenocarcinoma" data set available from The Cancer Genome Atlas website (54). *P*-values in (C) were determined by One-way ANOVA with Tukey's Multiple Comparison Test. * $P < 0.05$; ** $P < 0.01$; *** $P < 0.001$.

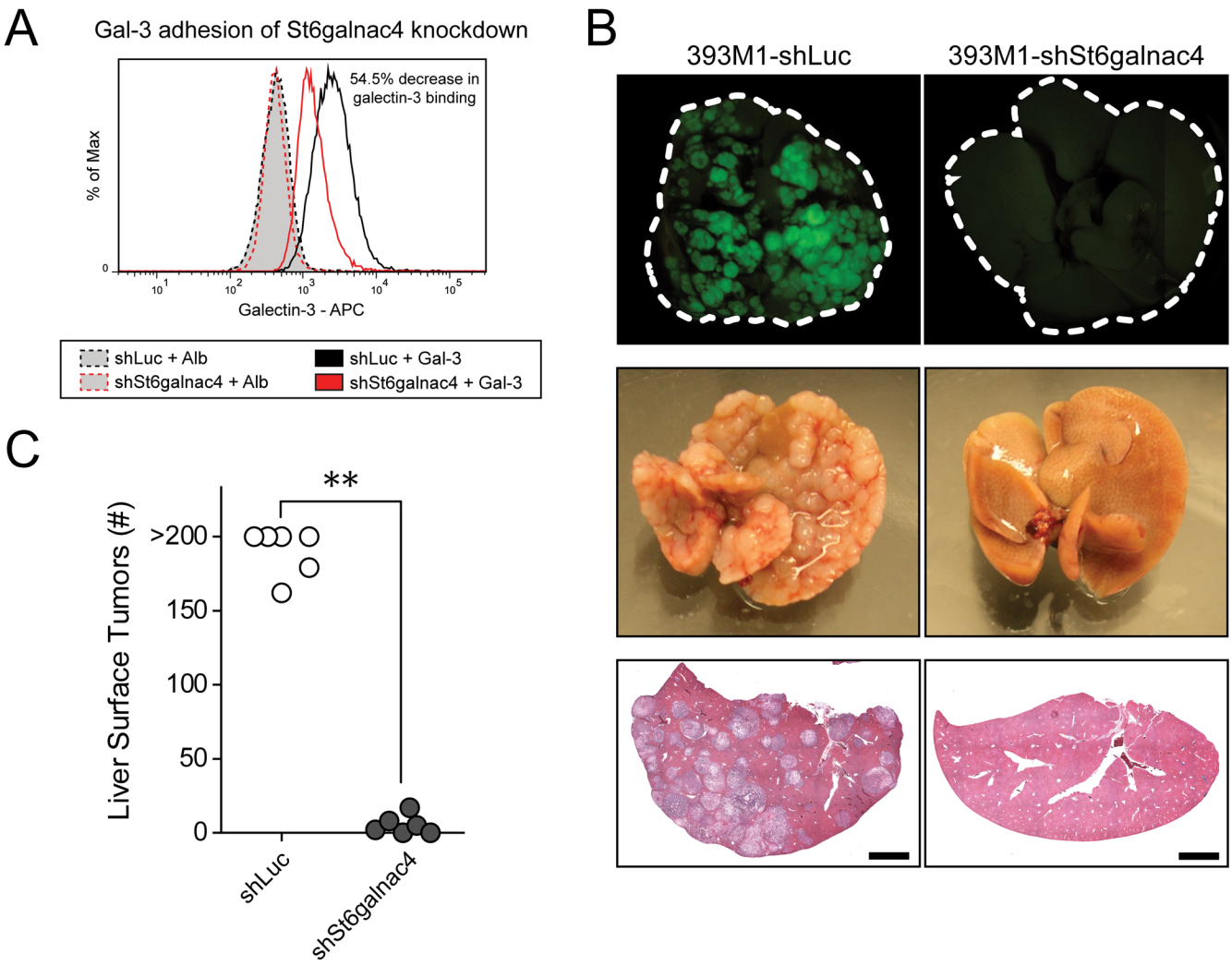

Figure 6. Knockdown of *St6galnac4* reduces galectin-3 binding and prevents metastasis *in vivo*

(A) Analysis of galectin-3 binding to the M line 393M1 following knockdown of *St6galnac4* by retroviral transduction of short hairpins targeting *St6galnac4* or a control gene (Luc, firefly luciferase) by flow cytometry. (E,F) Wild-type mice were transplanted with GFP^+ M cells bearing the short hairpin targeting *St6galnac4* (393M1-shSt6galnac4) or control hairpin (393M1-shLuc) by intrasplenic injection. Two weeks following implantation, the livers of mice were excised and imaged. (B) Representative livers as visualized by fluorescence (top), brightfield (middle), and hematoxylin and eosin staining (bottom). (C) Quantification of the number of surface nodules on the livers. Scale bars in (B) are 2mm. *P*-value in (C) was determined by Mann-Whitney test. ** $P < 0.01$.

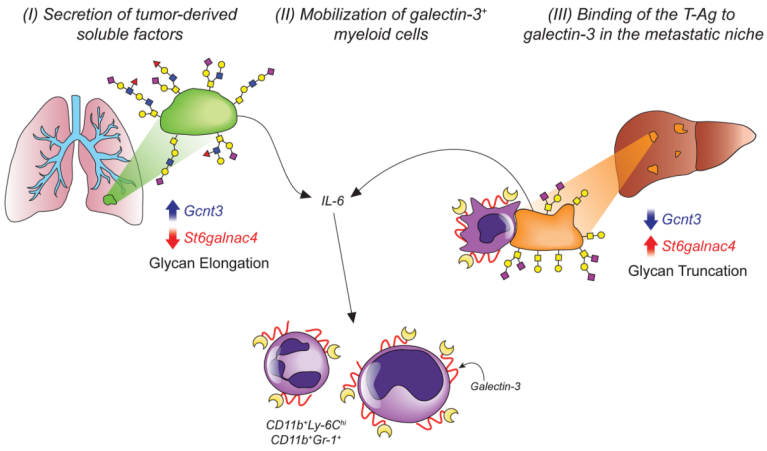

Figure 7. T-Antigen presentation promotes metastasis through interactions with galectins in the metastatic niche

Schematic model of galectin-glycan interactions in lung cancer metastasis. Primary lung tumors have high expression of branching glycosyltransferases such as C2GnT2 (*Gcnt3)* and low expression sialyltransferases such as St6GalNAcIV that act to promote *O*-glycan branching and elongation. Both the primary and metastatic tumors secrete tumor-derived soluble factors, such as IL-6, which act to mobilize $CD11b^{+}$galectin-3^{+} myeloid cells into the peripheral blood. Galectin-3 levels become elevated in the liver early metastatic niche where it is presented on macrophages. Metastatic cells adhere to galectin-3 and -8 through increased T-Antigen presentation, which is mediated by aberrant glycosyltansferase activity. Decreased expression of the branching transferases and increased expression of sialyltransferases prevent glycan elongation and promote preservation of the T-Antigen, which in turn, mediates galectin-3 adhesion.